International Journal of Engineering & Technology, 7 (4.11) (2018) 206-211

International Journal of Engineering & Technology

Website: www.sciencepubco.com/index.php/IJET

Research paper

Improving Low-Cost Solutions for Path Mapping in Autonomous Vehicle

Fadhlan Hafizhelmi Kamaru Zaman, Juliana Johari, Syahrul Afzal Che Abdullah, Nooritawati Md Tahir*

Faculty of Electrical Engineering, Universiti Teknologi MARA, 40450 Shah Alam, Selangor, Malaysia
**Corresponding author E-mail: nooritawati@ieee.org*

Abstract

One of the main challenge in designing autonomous vehicle is developing the algorithms necessary for simultaneous localization and mapping (SLAM). While this process heavily depends on an expensive hardware called Light Detection and Ranging (LiDAR), there are cheaper alternatives that can be implemented in earlier stage of autonomous vehicle development. Inertial Measurement Unit (IMU), vehicle odometry, and Global Positioning System (GPS) can be used as a solution. The main problem is these cheaper alternatives relies heavily on the precision of the hardware used. In this project, we outline the mapping process using these cheaper solutions which can also be used to complement LiDAR-based SLAM. We show that using simple approaches such as static bias drift removal, high-pass filtering, signal downsampling and linear interpolation, we can increase the robustness and improve the accuracy and precision of the IMU and GPS used respectively. We manage to increase the precision of the GPS readings and reduce the drift of IMU on average from -17.105 deg/min to -0.1177 deg/min. We show the improvement achieved by our proposed method by mapping the road around Engine Square, Jalan Ilmu 1/1, Universiti Teknologi MARA, Shah Alam, Selangor, Malaysia.

Keywords: *Inertial measurement unit; global positioning system; path planning; dead reckoning; autonomous vehicle.*

1. Introduction

Autonomous vehicle has received unprecedented attention by many, including researchers and manufactures alike. A lot of researches and billion of dollars are spent to achieve the elusive and highly complicated highest level of vehicle automation. The highest level of vehicle automation, called fully autonomous driving stood on level 5 of Society of Automotive Engineers (SAE) Autonomy Level [1]. It states that the vehicle should achieve mode-specific performance by an automated driving system of all aspects of the dynamic driving task under all roadway and environmental conditions that can be managed by a human driver.

To achieve such complex automation, the problem of autonomous driving can be divided into two individually separate tasks [2]. The first task focuses on keeping the vehicle moving along a nominal path while the second task focuses on the capability of the vehicle to perceive and react to unpredictable dynamic obstacles, like other vehicles, pedestrians, and traffic signalization. For the first task, autonomous vehicle must be equipped with an array of sensors, including Global Positioning System (GPS) receiver to locate GPS the coordinates of the vehicle, Inertial Measurement Unit (IMU) to compute the vehicle heading and Light Detection and Ranging (LiDAR) employed to detect the road shape or road infrastructures [3]. These sensors allow autonomous vehicle to accurately determine its position relative to the road limits. However, they are expensive and thus among the factors that lead to a very expensive price of an autonomous vehicle. Choosing cheaper alternatives of these sensors would compromise the navigation ability, since autonomous driving requires the precision must be in the order of few centimeters. Cheap sensors such as Global Navigation Satellite System (GNSS) for example does not reach this level of accuracy. According to [4], the accuracy of the civil GPS system is better than 7.8 m 95% of the time which is insufficient for accurate navigation. Thus, in this paper, we outline several methods that can be used to improve the accuracy and robustness of relatively cheaper solutions of these sensors.

Among the most common methods to improve IMU or gyro sensor readings are to integrate Inertial Navigation System (INS) and GPS information [5-7], and map-matching enhancement [8]. The main drawback is that they required external references or information ahead of time, which may not be available all the time. IMU measurements can also be processed through a conventional INS algorithm and are then integrated with high-sensitivity global positioning system (HSGPS) receiver measurements and dynamics derived constraint measurements using a tightly coupled integration strategy [9]. Besides, the Heuristic Drift Reduction (HDR) method is proposed in [10] to improve IMU or gyro sensors, where it computes the drift component and eliminates it, reducing heading errors by almost one order of magnitude. Since IMU and gyros are also sensitive to changes in temperature, in [2] suggests a compensation of the thermal bias in order to improve its readings.

On the other hand, there are several methods used previously to improve the accuracy of a GPS system by using correction signal provided by a base station which allows recalculation of the global position with up until few centimeters. Examples of this method are Differential GPS (DGPS) [11], Wide Area Augmentation System (WAAS) [12] and Real-Time Kinematic (RTK) [13]. The drawback of this method is it is not effective since the degradation of GPS signal is very severe in urban environment due to interference by buildings, limited sky view and multipath reflections.

The main contribution of this paper is the presentation on how to improve a relatively cheap sensor solutions using simple approaches such as combining two IMU sensors for a more robust change of heading measurement, removal of static bias drift from

IMU sensor readings, application of high-pass filter to remove drifts, and reconstruction of GPS coordinates by downsampling and linear interpolation to increase the precision of GPS receiver. The paper is organized as follows. Section 2 presents our proposed methods. Section 3 discusses the results obtained in several experiments and Section 4 concludes the paper.

2. Methodology

In this section we describe two strategies that can be used to improve the IMU and GPS receiver readings by (1) reducing the effect of drifting in IMU by static bias drift removal and (2) increasing the precision of GPS by signal downsampling and linear interpolation. We show that by using these relatively simple approaches, mapping of vehicle waypoints can be significantly improved, where the map waypoints are constructed using Dead Reckoning method to verify the effectiveness of the proposed method.

2.1. Static Bias Drift Removal

The change of direction when a vehicle is moving in its path can be denoted by rate of rotation around z-axes, or also denoted as angular displacement $\Delta\theta$. The measurement of this angular displacement can be made by integrating the instantaneous angular velocity at time t, $\omega(t)$ according in (1):

$$\Delta\theta = \int_{t}^{t+\Delta t} \omega(t)\, dt \tag{1}$$

Suppose that a vehicle is moving straight forward, the output of the z-axes and ideal IMU (i.e., the perfect IMU sensor that measures the change in heading when traveling on flat, horizontal ground) should be exactly zero throughout the trip, i.e. $\omega = 0$. However, that's not the case with actual IMU, where the vehicle heading will be off by some error ε due to drifts exist in the IMU. If the drift or bias value is not perfectly compensated, the path reconstruction by dead reckoning will suffer a bend [2]. Let ω_{true} be the true angular velocity of the vehicle, ε_0 is the static bias drift, and ε_d is the bias drift that is the difference between the static bias drift and the unknown near-DC drift component. The non-filtered angular velocity ω_{raw} can be expressed as a product of true angular velocity ω_{true} and the drifts, ε_0 and ε_d, as shown in (2):

$$\omega_{raw} = \omega_{true} + \varepsilon_0 + \varepsilon_d \tag{2}$$

To simplify, in this work, we assume that the random walk or bias drift $\varepsilon_d = 0$ such that the true angular velocity ω_{true} can be expressed in (3):

$$\omega_{true} = \omega_{raw} - \varepsilon_0 \tag{3}$$

The static bias drift ε_0 can be computed as average of ω_{raw} over time of τ seconds when the IMU sensor is held completely motionless [10]. τ is also called bias time, and its value depends on the quality of the IMU and can be estimated by using the IEEE Standard Specification Format Guide and Test Procedure for Single-Axis Interferometric Fiber Optic Gyros [14]. In this work, we use the InertialSense® uAHRS miniature attitude heading reference system module and InertialSense® miniature magnetic mount GPS/GLONASS Antenna for GPS data collection. This is shown in Fig. 1. For the IMU used in our work, $\tau = 100$ seconds is used, as obtained from Allan Deviation plot given in Fig. 2.

$$\varepsilon_0 = \frac{1}{\tau}\sum_{t=1}^{\tau} \omega_{raw}(t) \tag{5}$$

Taking that the actual change in vehicle direction $\Delta\theta$ can only be computed correctly and precisely using the true angular velocity ω_{true}, in (1) becomes:

$$\Delta\theta = \int_{t}^{t+\Delta t} (\omega_{raw}(t) - \varepsilon_0)\, dt \tag{6}$$

Fig. 1: The InertialSense® uAHRS miniature attitude heading reference system module (on the left) used for inertial measurement, and InertialSense® miniature magnetic mount GPS/GLONASS Antenna (on the right) used in GPS data collection for distance estimation

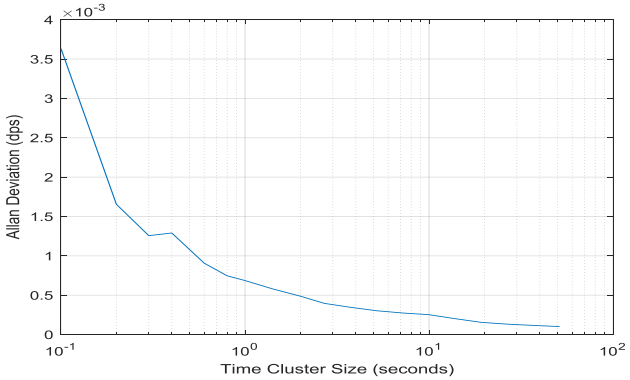

Fig. 2: Allan deviation plot for InertialSense® uAHRS miniature IMU used in this work. The bias stabilizes approaching $\tau = 100$ seconds

The InertialSense® uAHRS used in this work contains two individual IMU sensors, namely sensor 1 and sensor 2. The angular velocity attributed to these sensors are denoted as $\omega_{z,1}$ and $\omega_{z,2}$ which are angular velocities from sensor 1 and sensor 2 readings, respectively. The drifts of these sensors can be shown as individual reading of angular velocity of $\omega_{z,1}$ and $\omega_{z,2}$ when the IMU is put in motionless state (idle). This is shown in Fig. 3. Based on Fig. 3, $\omega_{z,1}$ and $\omega_{z,2}$ indicates there are motions around z-axes detected by the IMU, where in truth the IMU is idle. This is a perfect indication that the $\omega_{z,1}$ and $\omega_{z,2}$ readings are due to drifts in the IMU.

We combine both the angular velocities $\omega_{z,1}$ and $\omega_{z,2}$ as total angular velocity ω_{raw} by a weighted approach for a more robust sensor output. Let k denotes the combination weight, the angular velocity ω_{raw} as a function of angular velocity from sensor 1 and angular velocity from sensor 2, $\omega_{z,1}$ and $\omega_{z,2}$ can be computed in (7):

$$\omega_{raw} = \frac{(2-k)\,\omega_{z,1} + k\omega_{z,2}}{2}, \quad where\ 0 \le k \le 2 \tag{7}$$

Based on (7), if $k = 0$, only $\omega_{z,1}$ is used as ω_{raw}, while if $k = 2$, only $\omega_{z,2}$ is used as ω_{raw}. $k = 1$ equally computes $\omega_{z,1}$ and $\omega_{z,2}$ as ω_{raw}. Combining in (6) and (7) yields:

$$\Delta\theta = \int_{t}^{t+\Delta t} \left(\frac{(2-k)\,\omega_{z,1}(t) + k\omega_{z,2}(t)}{2} - \varepsilon_0 \right) dt \tag{8}$$

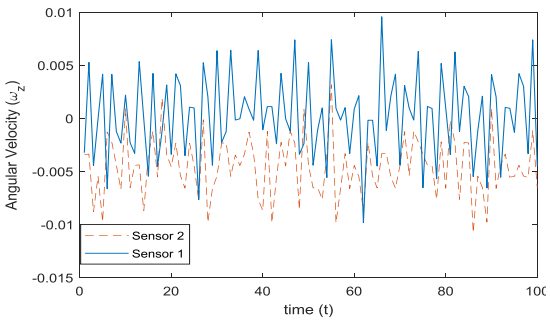

Fig. 3: Drifts shown as angular velocities (ω_z) produced by both IMU sensor 1 and sensor 2 when the sensors are idle

Based on the assumption that most of the time, the IMU sensors are in idle, and the change in direction is solely attributed to the drift inside the sensor itself. Thus, in this work, a high-pass filter is applied to remove very small motions detected by the IMU by assumption that those motions are actually caused by drifts. Let h be the threshold of the filter, the value of angular velocity ω_{raw} is computed in (9):

$$\omega_{raw} = \begin{cases} \omega_{raw} & if\ abs\ (\omega_{raw}) \geq h \\ 0 & if\ abs\ (\omega_{raw}) < h \end{cases} \quad (9)$$

2.2. Downsampling and Interpolation of GPS coordinates

In this work, InertialSense® miniature magnetic mount GPS/GLONASS Antenna operating at 10 Hz is used to collect GPS coordinates. As in relatively cheap GPS receivers, the precision of the GPS coordinates collected is not up to a standard that will allow autonomous navigation of a driverless car. The points are less accurate and tend to scatter around near proximities of the actual GPS points, drifting from the actual position. This problem is more apparent near trees and buildings, since the GPS signal are exposed to interferences. This problem is illustrated in Fig. 4.

Fig. 4: The map shows the actual GPS coordinates collected during experiment. Shown inset is the magnified view, highlighting the GPS precision's problem, where the point is not precisely on the path travelled by the vehicle. The problem is more apparent near tall buildings and trees

To improve the precision of the GPS coordinates, first we downsample the GPS signals to keep only every M^{th} sample of the original signal. We choose $M = 10$, thus the sampling is performed at a period of every 1 second for a 10Hz sensor. Let $\varphi_{lat,lon}$ denotes the latitude and longitude coordinates of the GPS point collected. The downsampled GPS signals into new time domain, u, can be expressed as $\varphi'_{lat,lon}(u)$. Then, we further remove cluster of GPS points located too close to each other at a distance interval $\Delta L < 3$ meters such that:

$$\varphi''_{lat,lon}(u) = \begin{cases} \varphi'_{lat,lon}(u), & if\ \Delta L < 3 \\ removed, & if\ \Delta L \geq 3 \end{cases} \quad (10)$$

After that, we perform interpolation to reconstruct the original signal. Simple linear interpolation is employed to reconstruct the signal removed by sampling processes. Linear interpolation is implemented by taking two sets of continuous GPS coordinates, $\varphi''_{lat,lon}(u)$ and $\varphi''_{lat,lon}(u-1)$. The reconstructed GPS coordinates, $\varphi_{lat,lon}$ can be found from (11):

$$\varphi_{lat,lon}(t) = \varphi''_{lat,lon}(u-1) + (t - t(u - 1)) \frac{\varphi''_{lat,lon}(u) - \varphi''_{lat,lon}(u-1)}{t(u) - t(u-1)} \quad (11)$$

2.3. Dead Reckoning

To visualize the improvement gained by applying our proposed methods, we map an actual road around Engine Square, Jalan Ilmu 1/1, Universiti Teknologi MARA, Shah Alam, Selangor, Malaysia using an actual car. The actual path is shown in Fig. 5. The IMU and GPS sensors are attached to the car, and the path taken by the vehicle are constructed by Dead Reckoning approach. Let the GPS receiver readings consisting of latitude, lat and longitude, lon at time t be denoted as $\varphi_{lat,lon}(t)$ and radius of earth, r = 6371 km. The distance interval ΔL (in km) can be computed in (12)-(14):

$$\varphi_{lat,lon}(t) = \varphi_{lat,lon}(t) \frac{\pi}{180} \quad (12)$$

$$\Delta\varphi_{lat,lon} = \varphi_{lat,lon}(t) - \varphi_{lat,lon}(t-1) \quad (13)$$

$$\Delta L = r \sqrt{\left[\Delta\varphi_{lon}\ cos\left(\frac{\varphi_{lat}(t) + \varphi_{lat}(t-1)}{2}\right)\right]^2 + \Delta\varphi_{lat}{}^2} \quad (14)$$

where θ is the yaw angle measured with respect to the y-axis, as illustrated in Fig. 6. The equations are executed in the frequency of 10 Hz, which means that at 30 km/h the linear increments will be of 0.83 m. Small linear increments are desirable because they are associated with small angular increments. This allows good description of curves by small straight sections and leads to the simplified Equations (15) – (17).

The dead reckoning computation is performed by the state transition Equations given in (15) – (17). Given the current vehicle's pose ($s_t = [x_t, y_t, \theta_t]^T$), the future pose s_{t+1} after a linear and angular displacement is computed by:

$$x_{t+1} = x_t + \Delta L\ sin(\theta_t + \Delta\theta/2) \quad (15)$$

$$y_{t+1} = y_t + \Delta L\ cos(\theta_t + \Delta\theta/2) \quad (16)$$

$$\theta_{t+1} = \theta_t + \Delta\theta \quad (17)$$

Fig. 5: The map shows the actual path (marked by blue marker) taken by a car for experiments conducted in this paper. The mapping was carried out around Engine Square, Jalan Ilmu 1/1, Universiti Teknologi MARA, Shah Alam, Selangor, Malaysia

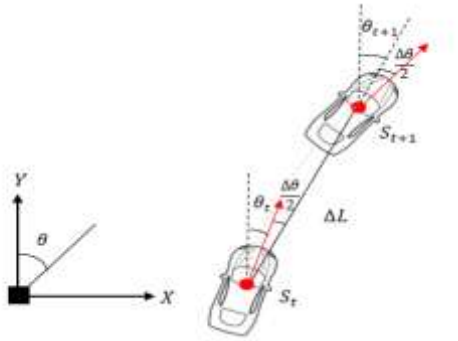

Fig. 6: Vehicle's state reference system.

3. Results and Discussion

In this section, we show some results obtained from the implementation of our proposed method. Signals from IMU and GPS are recorded while the mapping of actual vehicle path is carried out to validate our result. We highlight the results on drift reduction, GPS signal reconstruction, and result of mapping by Dead Reckoning approach. All experiments are carried out around Engine Square, Jalan Ilmu 1/1, Universiti Teknologi MARA, Shah Alam, Selangor, Malaysia using InertialSense® uAHRS miniature attitude heading reference system module and InertialSense® miniature magnetic mount GPS/GLONASS Antenna attached to a car moving on average 30 km/h.

3.1. Drift Reduction

Using (7), we combine the angular velocities acquired from both IMU sensors to produce a more stable change in direction and to reduce the effect of drifting. Two runs of experiments are performed, where in each run, the combination weight, k is varied from 0 to with 0.01 increments, and for each increment, 10000 sensor readings are recorded. The change of orientation is then computed in (8), where static bias drift ε_0 is assumed to be 0. Initially, the orientation is set to be heading in 90-degree direction. The resulting orientation change is shown in Fig. 7.

Based on results obtained from Fig. 7, the value of the best value of k for first run is k = 1.31, while second run is k = 1.54. This indicates that for each individual run, the best combining weight is not constant and might be changing. This is due to the randomness of the static bias drift and bias drift components in the IMU. Further, the drift in orientation can be severely affected by a non-careful selection of the weight, k. In Fig. 8, it is shown that selection of k at two extremities of $k = 0$ and $k = 2$, would yield a more severe drift. It also shows that utilizing individual sensor may also produces worse results. Better sensor output robustness is observed from using combination of both sensors. Thus, throughout this paper, otherwise stated, we chose k = 1.54 for all experiments since it provides less severe combined effect on drifting of Sensor 1 and Sensor 2.

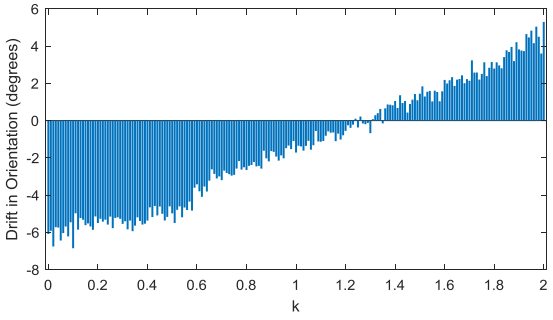

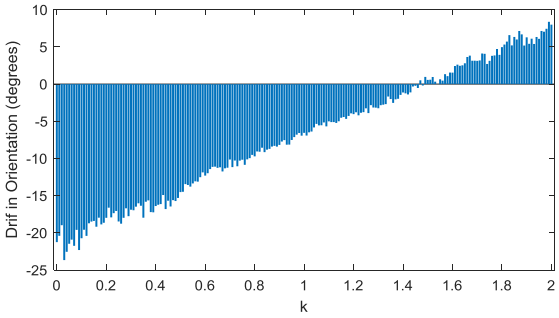

Fig. 7: Final drift (displacement) from the origin orientation (in 90 degrees direction) as a result of using different values of k for first run (top) and second run (bottom). The best value of k for first run is k = 1.31, while second run is k = 1.54

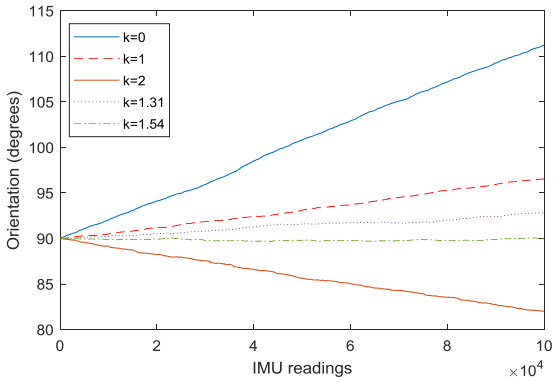

Fig. 8: Drift in orientation acquired in second run, using various values of k, including k = 0, k =1, k = 2 and the best k for second run, k = 1.54. Shown together is the orientation acquired from k = 1.31.

After that, high-pass filter with threshold h = 0.01 is applied to the IMU sensor readings, such as outlined in (9). Based on Fig. 9, for an experimental run of 100 seconds, the high-pass filtering can further reduce the drift of the IMU. This is due to the ability of the filter to exclude small sensor readings which are assumed to be attributed to drifts. Another method of removing drift is by applying static bias drift removal method as described by in (6). Besides high-pass filtering, the static bias drift ε_0 is first approximated by using in (5) and the resulting $\varepsilon_0 = 0.00437$ is deducted from each angular velocity measured. The result from this implementation is shown in Fig. 10. The resulting orientation is now less affected by the drift, where the change in orientation is now reduced.

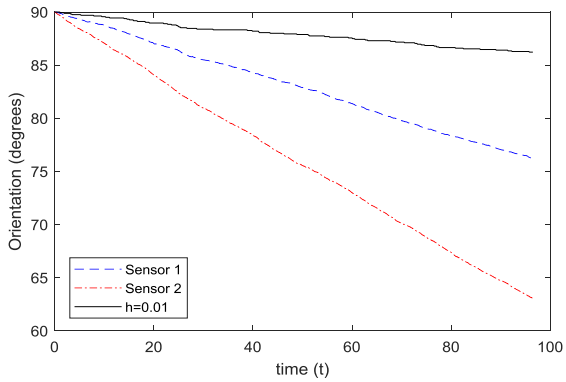

Fig. 9: Drift in orientation acquired using high-pass filter, where h = 0.01.

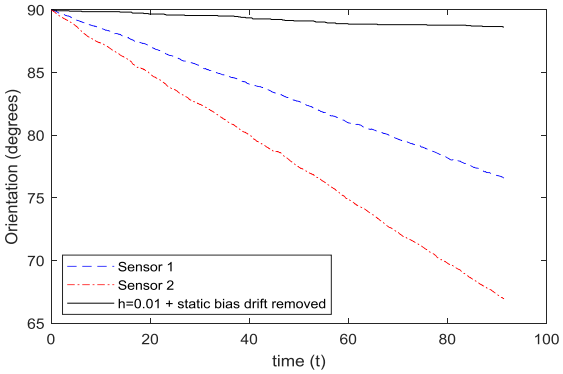

Fig. 10: Drift in orientation acquired using static bias drift removal, where $\varepsilon_0 = 0.00437$

Furthermore, 10 experimental runs for each implementation described earlier is carried out to measure the resulting drift in Average Drift measured in degree per minute (°/min). The results are tabulated in Table 1. Based on results in Table 1, the average drift obtained for when only Sensor 1 is used is -7.1761 °/minwhile Sensor 2 yields -17.105 °/min. The combination of both sensors yields a drift of -14.178 °/min. While this drift is significantly more severe than Sensor 1, it is better than the average drift of Sensor 2. During actual usage if the IMU sensors, we may not know which sensor will produce larger drifts, thus it is more sensible to combine the readings from both to reduce the drift effects.

Table 1: Average drift calculated over 10 trials for different approaches of drift reduction

Drift Removal Techniques	Average Drift (°/min)
Baseline Sensor 1	-7.1761
Baseline Sensor 2	-17.105
Baseline Combined Sensors	-14.178
Combined Sensors + high-pass filter	-2.8894
Combined Sensors + ε_0 removed	**-0.1177**
Combined Sensors + ε_0 removed + high-pass filter	-1.7068

The average drift for high-pass filtering further improves the average drift to -2.8894 °/min. Although this seems a very large improvement, the drift is still unacceptable for autonomous navigation. The static bias removal reduces the drift further to just -0.1177 °/min while implementation of static bias drift removal on high-pass filtered signal yields average drift of -1.7068 °/min. This is actually worse than static bias removal only implementation. Thus, we suggest that high pass filtering can only be applied in combined sensors approach without removal of static bias drift. The reason is the application of high-pass filter sometimes falsely remove the actual motions and not just the drifts.

3.2. GPS Coordinates Reconstruction

Using downsampling approach and cluster removal describe in (10), the GPS coordinates reading are reduced to less points. This is to remove the imprecision of the original coordinates. After this removal, linear interpolation is applied so that the GPS coordinates are reconstructed to its original signal, but with imprecisions removed. This strategy is shown in Fig. 11.

According to Fig. 11, the base outline of the GPS coordinates is left unchanged. However, the imprecise points are now effectively removed. This is very important, since the computation of vehicle path from Dead Reckoning approach heavily relies on the precision of interval distance estimation. Slight inaccuracies of the estimations will lead to the vehicle steering away from its intended path. As a result, the imprecise GPS coordinates as shown in Fig. 5, is now improved as shown in Fig. 12. Based on Fig. 12, the reconstructed coordinates are now more precise and smoother, especially around corners and places where GPS signals are mostly interrupted and interfered.

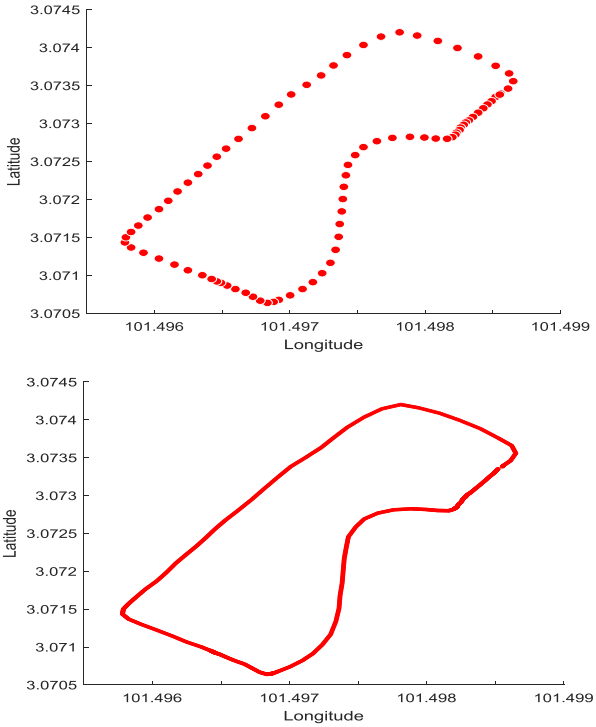

Fig. 11: To reduce the effect of imprecision in GPS readings, raw GPS points is downsampled and filtered to remove the inaccurate points such that less points are left (shown at the top) before it is being up-sampled by mean of linear interpolation (shown at the bottom)

3.3. Mapping by Dead-Reckoning Approach

To verify the effectiveness of our proposed methods in improving the IMU and GPS sensors readings, an experimental run of actual vehicle driven around actual road is carried out. The road path is shown in Fig. 5. The IMU and GPS sensors are attached to a car, and the car is driven around the specified path 2 times. The first run is the baseline run, which validates the drift effects when no drift removal or GPS reconstruction method is applied. On the other hand, second run implements our proposed static bias drift removal and GPS coordinates reconstruction. The resulting map waypoints are constructed using Dead Reckoning approach as outlined in (12) – (17). The maps acquired from these 2 runs are illustrated in Fig. 13 and Fig. 14 respectively.

Fig. 12: The map shows the improved GPS coordinates points from our proposed method. Inset images show that the problem of imprecision with GPS sensor readings now has been significantly reduced

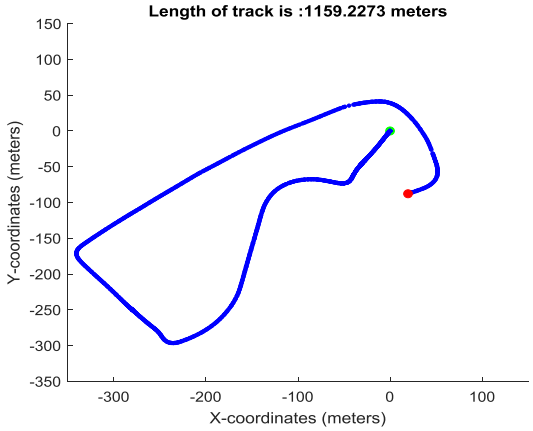

Fig. 13: The map shows the IMU dead-reckoning points without any drift removal or GPS reconstruction applied. Inset image shows the difference of start (green) and end (red) points which is caused by drift which significantly affect the precision of the mapped path

According to Fig. 13, the map waypoints constructed from dead reckoning shows a very severe drift and heavily bent. This is indicated by the misalignment of the start and end points on the map and the bend of the waypoints curvature as compared to actual waypoints. The actual car travels from starting point and end exactly at the same spot. For ideal sensors without any drift and imprecision, the waypoints should be similar to the map shown in Fig. 5. The drift in IMU and imprecision of GPS coordinates cause the reconstructed waypoints to be departing from the actual path, causing the end point to appear on the map significantly further away from the starting point.

Based on Fig. 14, significant improvement in waypoints precision is acquired due to combination of IMU sensors and removal of static bias drift. The end point and the starting point of the map is on separated away by 5 meters. This due to the imprecision of the actual vehicle stopping point on the map. The effect of drift is reduced, and the drifting only causes the waypoints to depart at the end point by 1 meter. This shown clearly in Fig. 14, by a dashed red line indicating where the actual waypoints should be for ideal sensor with 0 drift. The slight drifting is actually due to the random walk or bias drift $\varepsilon_d$which is unaccounted for in this work. To remove this drift will require additional work which will be discussed in the future.

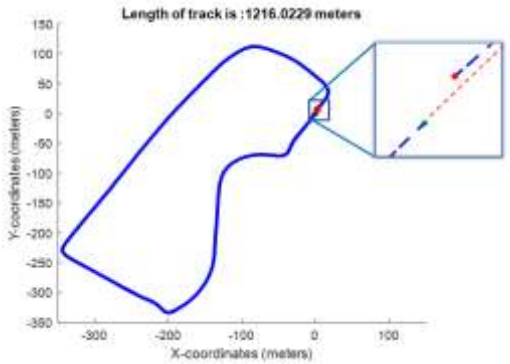

Fig. 14: The map shows the improved IMU dead-reckoning points from combined IMU sensor + static bias drift removed. Inset image shows the difference of start (green) and end (red) points which is caused by drift which is reduced significantly by the proposed method. Red dashed line indicates the path that supposed to be mapped in ideal sensor condition (0 drift)

4. Conclusion

The paper discusses on several methods to improve low-cost solutions for autonomous vehicle path mapping. The methods presented here includes combining two IMU sensors for a more robust change of heading measurement, removal of static bias drift from IMU sensor readings, application of high-pass filter to remove drifts, and reconstruction of GPS coordinates by downsampling and linear interpolation to increase the precision of GPS receiver. Results obtained from experiments suggest that these methods can improve the robustness and the accuracy of the sensors. Validation of the proposed methods effectiveness by actual vehicle mapping shows that the constructed map is significantly improved, by reducing the departure of mapped waypoints from the actual waypoints. The methods can be improved further by taking into consideration the random walk or bias drift component $\boldsymbol{\varepsilon_d}$ in the sensor readings.

Acknowledgement

This research is funded by Institute of Research Management and Innovation (IRMI), Universiti Teknologi MARA (UiTM), Shah Alam, Selangor, Malaysia under the Research Grant Scheme No: 600-RMI/DANA 5/3/PSI (195/2013) and Faculty of Electrical Engineering UiTM Shah Alam for all the support given during this research.

References

[1] Wayback Machine, 2017.
[2] R. Vivacqua, R. Vassallo, and F. Martins, "A low cost sensors approach for accurate vehicle localization and autonomous driving application," Sensors, 17(10), 1-33, 2017.
[3] O. Wulf and B. Wagner, "Fast 3D scanning methods for laser measurement systems," Proceedings of the International Conference on Control Systems and Computer Science, 2003, pp. 2-5.
[4] GPS.gov, "GPS accuracy," 2016, http://www.gps.gov/systems/gps/performance/accuracy/.
[5] F. Cavallo, A. M. Sabatini, and V. Genovese, "A step toward GPS/INS personal navigation systems: Real-time assessment of gait by foot inertial sensing," Proceedings of the IEEE/RSJ International Conference on Intelligent Robots and Systems, 2005, pp. 1187-1191.
[6] M. S. Grewal, L. R. Weill, and A. P. Andrews, Global positioning systems, inertial navigation, and integration. John Wiley and Sons, 2007.
[7] G.-B. D.A., T. C., S. Moafipoor, Y. Jwa, and J. Kwon, "Multi-sensor personal navigator supported by human motion dynamics model," Proceedings of the 3rd IAG Symposium on Geodesy for Geotechnical and Structural Engineering/12th FIG Symposium on Deformation Measurements, 2006, pp. 129-140.
[8] C. Basnayake, O. Mezentsev, G. Lachapelle, and M. E. Cannon, "An HSGPS, inertial and map-matching integrated portable vehicular navigation system for uninterrupted real-time vehicular navigation," International Journal of Vehicle Information and Communication Systems, 1(1-2), 131-151, 2005.
[9] S. Godha and G. Lachapelle, "Foot mounted inertial system for pedestrian navigation," Measurement Science and Technology, 19(7), 1-9, 2008.
[10] J. Borenstein, L. Ojeda, and S. Kwanmuang, "Heuristic reduction of gyro drift in IMU-based personnel tracking systems," Optics and Photonics in Global Homeland Security V and Biometric Technology for Human Identification VI, 2009, 7306, 1-11.
[11] P. Misra and P. Enge, Global positioning system: Signals, measurements and performance. Jamuna Press, 2006.
[12] Y.-C. Chao, "Real time implementation of the wide area augmentation system for the global positioning system with an emphasis on ionospheric modeling," PhD theis, Stanford University, 1997.
[13] B. M. Scherzinger, "Precise robust positioning with inertially aided RTK," Navigation, 53(2), 73-83, 2006.
[14] Institute of Electrical and Electronics Engineers (IEEE), IEEE standard specification format guide and test procedure for single-axis interferometric fiber optic gyros. IEEE, 1996.